

A Composite Spectral Model and Its Applications

Yinlong Sun
Department of Computer Sciences, Purdue University, West Lafayette, IN, 47907-1398, USA
sun@cs.purdue.edu

F. David Fracchia
Mainframe Entertainment, 500-2025 West Broadway, Vancouver, BC, Canada, V6J 1Z6
drdude@reboot.com

Mark S. Drew
School of Computing Science, Simon Fraser University, Burnaby, BC, Canada, V5A 1S6
mark@cs.sfu.ca

Abstract

A new spectral representation called the *composite model* is proposed. Its key point is to decompose all spectra into a smooth background and a collection of spikes. The smooth part can be represented by Fourier coefficients and a spike by its location and height. In this paper, the sufficiency of a low-dimensional representation is shown analytically based on the characteristics of human perception. A re-sampling technique is also proposed to improve performance. The composite model demonstrates advantages in all identified representation criteria including accuracy, compactness, computational efficiency, portability and flexibility. Its applications in areas of realistic image synthesis, image understanding, storage and communication of spectral images, and deriving natural spectra are discussed.

Keywords: Spectra, representation, color, applications.

Introduction

Spectral functions, including spectral power distributions (SPDs), reflectances and transmittances, are an essential concept in image synthesis, image understanding, and color science. Natural spectra may have arbitrary shapes; some are smooth and others are spiky, as shown in Figure 1. Mathematically they require an infinite number of parameters to describe exactly. In practice, however, describing every spectrum with a large number of parameters is not feasible, because a real view usually involves hundreds or even thousands of spectral functions. Therefore, it is highly desirable that all spectra be represented through a small number of parameters while maintaining sufficient accuracy.

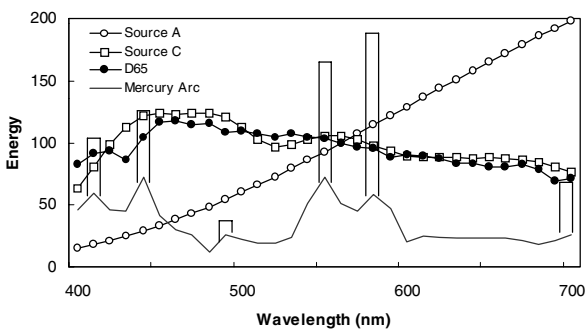

Figure 1: The SPDs of some real light sources.

Overall, the following criteria should be considered for spectral representations:

1. *Accuracy*: Since a practical spectral representation always involves some approximation, it is essential to provide an appropriate measurement of accuracy to ensure that errors are reasonably bounded.
2. *Compactness*: While maintaining a sufficient accuracy, spectra should be represented with as few parameters as possible, because the compactness is useful in saving the required space for storing spectral data.
3. *Performance*: Fast computations are always desired. In many cases, the overall performance efficiency is largely determined by the efficiency of multiplying two spectra, as shown in Eq. (1), because this computation is associated with each reflection and transmission.
4. *Portability*: A representation should be uniform in format across applications. Although transforming one representation to another can be trivial in some applications [2], in general the work can be very laborious. Considering a situation in image synthesis when one uses many graphical models (such as a copper vase, plants, etc.) created using different spectral formats, unifying the graphical models can be a significant bottleneck.
5. *Flexibility*: A representation should be flexible in the sense that one can easily adjust it to meet specific application requirements. For example, accuracy is a priority in realistic image synthesis while performance efficiency is more important in real-time applications.

In previous representations [16], sampling is most commonly used. This method can obtain very high accuracy if a large number of sample points are used, and achieve linear performance for spectral multiplications

$$S_3(\lambda_i) = S_1(\lambda_i)S_2(\lambda_i), \quad i = 1,..., N, \tag{1}$$

where $\lambda_1,...,\lambda_N$ are N sampled wavelengths. Sampling is also portable because its data are straightforward, and flexible because tradeoffs between accuracy and speed can be easily made by choosing different N. Its disadvantage is poor compactness; in particular, many sample points are needed to represent fluorescent SPDs because such spectra contain very narrow peaks, of widths under 1 nm typically. Another popular representation method is the linear model, which expresses a spectrum as a linear combination of a set of basis functions. Usually the basis functions are derived numerically so that they can best represent all spectra within a specified domain [6, 12, 14]. The linear model is fairly

accurate, compact and flexible. However, its spectral multiplication is $O(M^2)$, where M is the number of basis functions, which is relatively computationally expensive. Besides, the linear model is not very portable because exporting a spectrum requires not only the coefficients, but also the basis functions (otherwise the coefficients are meaningless). Spectra can also be represented with polynomials [7, 15] and the polynomial degree determines the compactness. Its problem is that it cannot accurately represent spectra with abrupt peaks such as in fluorescent SPDs. It is also not very efficient because spectral multiplication is $O(M^2)$, where M is the polynomial degree. Although portable, it is not flexible: if we change the polynomial degree, all the coefficients have to be recomputed to find the best fit. These previous methods are summarized in Table 1.

Table 1: Comparing different spectral representations. The "Yes" and "No" roughly indicate whether or not they meet the corresponding criterion.

	Sampling	Linear model	Polynomial	Composite model
Accuracy	Yes	Yes	No	Yes
Compactness	No	Yes	Yes	Yes
Efficiency	Yes	No	No	Yes
Portability	Yes	No	Yes	Yes
Flexibility	Yes	Yes	No	Yes

This paper proposes a new spectral representation method called the *composite model* [18]. Its key point is to decompose any spectrum into a smooth background and a collection of spikes. The smooth part can be represented by Fourier coefficients and a spike by its location and height. Based upon the characteristics of human perception, we will show that it is possible to represent spectra with a small number of parameters. To improve performance, we propose re-sampling the smooth part that is reconstructed from Fourier coefficients, and as a result the computational complexity is greatly reduced. The composite model improves upon the existing methods with aspect to the identified criteria. It has promise in a number of application areas including image synthesis, image understanding, storage and communication of spectral images, and deriving natural spectra.

Composite Model

Basic Idea

In the composite model, any spectrum is decomposed into a smooth background and a collection of spikes

$$S(\lambda) = S_{\text{smooth}}(\lambda) + S_{\text{spikes}}(\lambda), \tag{2}$$

where

$$S_{\text{spikes}}(\lambda) = \sum_{m=1}^{M} w_m \delta(\lambda - l_m), \tag{3}$$

where l_m and w_m denote the location and weight (or height) of a spike, and the smooth part can be expressed by a Fourier transform over the visible range $[\lambda_{\min}, \lambda_{\max}]$

$$S_{\text{smooth}}(\lambda) = \frac{a_0}{2} + \sum_{n=1}^{\infty}\left\{a_n \cos\left[\frac{2\pi n(\lambda-\lambda_{\min})}{L}\right] + b_n \sin\left[\frac{2\pi n(\lambda-\lambda_{\min})}{L}\right]\right\}, \tag{4}$$

where $L = \lambda_{\max} - \lambda_{\min}$ and

$$\begin{cases} a_n = \dfrac{2}{L}\displaystyle\int_{\lambda_{\min}}^{\lambda_{\max}} S_{\text{smooth}}(\lambda)\cos\left[\frac{2\pi n(\lambda-\lambda_{\min})}{L}\right]d\lambda \\ b_n = \dfrac{2}{L}\displaystyle\int_{\lambda_{\min}}^{\lambda_{\max}} S_{\text{smooth}}(\lambda)\sin\left[\frac{2\pi n(\lambda-\lambda_{\min})}{L}\right]d\lambda \end{cases} \tag{5}$$

for $n = 0,1,2,...,\infty$. Note that a smooth spectrum is dominated by low-frequency components. If we ignore all the coefficients with indices above N, the spectrum can be represented approximately with the lowest $2N+1$ Fourier coefficients $a_0,...,a_N$ and $b_1,...,b_N$. (Note that $b_0 = 0$.)

Sufficiency of a Low-Dimensional Representation

Given any smooth function $S_{\text{smooth}}(\lambda)$, its corresponding color in CIE XYZ space is given by

$$X_k = \kappa \int_{\lambda_{\min}}^{\lambda_{\max}} S_{\text{smooth}}(\lambda)\bar{x}_k(\lambda)d\lambda, \quad k = 1,2,3 \tag{6}$$

where $\bar{x}_k(\lambda)$ are the CIE XYZ color matching functions and κ is a constant. (We drop κ below as this does not affect the relative accuracy.) Substituting Fourier transformations for both $S_{\text{smooth}}(\lambda)$ and $\bar{x}_k(\lambda)$ into Eq. (6), we have

$$X_k = \frac{a_0\bar{a}_{0,k}}{4} + \sum_{n=1}^{\infty}[a_n\bar{a}_{n,k} + b_n\bar{b}_{n,k}], \quad k = 1,2,3 \tag{7}$$

where a_n and b_n are the Fourier coefficients of $S_{\text{smooth}}(\lambda)$, and $\bar{a}_{n,k}$ and $\bar{b}_{n,k}$ are those of $\bar{x}_k(\lambda)$. Eq. (7) has an important implication: *if the high-frequency coefficients of either $S_{\text{smooth}}(\lambda)$ or $\bar{x}_k(\lambda)$ are negligibly small, we can represent $S_{\text{smooth}}(\lambda)$ through its low-frequency Fourier coefficients while maintaining good accuracy*.

To show this is the case, let us describe $\bar{x}_k(\lambda)$ with

$$g(\lambda) = he^{-4(\ln 2)(\lambda-\lambda_c)^2/w^2}, \tag{8}$$

where parameters h, λ_c, and w correspond to the height, center, and width (at half height) of a Gaussian function, respectively, such that $\bar{x}_k(\lambda)$ are approximated as

$$\begin{cases} \bar{x}_1(\lambda) \approx h_{1a} e^{-4(\ln 2)(\lambda-\lambda_{c,1a})^2/w_{1a}^2} + h_{1b} e^{-4(\ln 2)(\lambda-\lambda_{c,1b})^2/w_{1b}^2} \\ \bar{x}_2(\lambda) \approx h_2 e^{-4(\ln 2)(\lambda-\lambda_{c,2})^2/w_2^2} \\ \bar{x}_3(\lambda) \approx h_3 e^{-4(\ln 2)(\lambda-\lambda_{c,3})^2/w_3^2}. \end{cases} \quad (9)$$

Good fitting parameter values are displayed in Table 2, and Figure 2 shows a good correspondence between the original and fitted curves.

Table 2: Fitting Parameters for the CIE color matching functions.

Small peak of $\bar{x}_1(\lambda)$	$\lambda_{c,1a}$ = 445 nm	w_{1a} = 45 nm	h_{1a} = 0.38
Large peak of $\bar{x}_1(\lambda)$	$\lambda_{c,1b}$ = 595 nm	w_{1b} = 80 nm	h_{1b} = 1.06
$\bar{x}_2(\lambda)$	$\lambda_{c,2}$ = 560 nm	w_2 = 100 nm	h_2 = 1.0
$\bar{x}_3(\lambda)$	$\lambda_{c,3}$ = 451 nm	w_3 = 55 nm	h_3 = 1.8

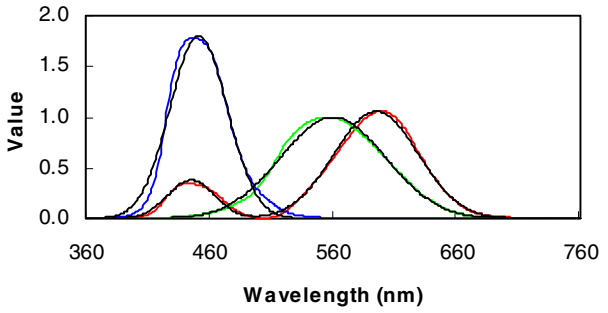

Figure 2: The red, green and blue curves are the original CIE color matching functions, and the black curves are fitted results.

Thus the Fourier coefficients of the CIE color matching functions can be calculated analytically (see Appendix):

$$\begin{cases} \bar{a}_{n,k} = \dfrac{\sqrt{\pi} h_k w_k}{\sqrt{\ln 2} L} \cos\left[\dfrac{2\pi n(\lambda_{c,k} - \lambda_{\min})}{L}\right] e^{-\pi^2 n^2 w_k^2/4(\ln 2)L^2} \\ \bar{b}_{n,k} = \dfrac{\sqrt{\pi} h_k w_k}{\sqrt{\ln 2} L} \sin\left[\dfrac{2\pi n(\lambda_{c,k} - \lambda_{\min})}{L}\right] e^{-\pi^2 n^2 w_k^2/4(\ln 2)L^2} \end{cases} \quad (10)$$

for $k = 2,3$, and similar results hold for $k = 1$. These results show that the Fourier coefficients vanish rapidly, in the speed of $\exp(-cn^2)$, where c is independent of n.

For a smooth spectrum, it is safe to assume that

$$a_n \propto \frac{1}{n}, \quad b_n \propto \frac{1}{n}. \quad (11)$$

For most natural smooth spectra a_n and b_n vanish much faster than $1/n$, and only for a few types of spectra, such as a step function or a linear function with a non-zero slope, a_n and b_n vanish exactly in the speed of $1/n$.

Based on Eqs. (10) and (11), the ratio of a term in the summation in Eq. (7) to the first is

$$\frac{4 \mid a_n \bar{a}_{n,k} \mid}{a_0 \bar{a}_{0,k}} \le \frac{4}{n} e^{-\pi^2 n^2 w_k^2/4(\ln 2)L^2}, \quad k = 2,3 \quad (12)$$

and similar inequalities hold for other terms. With L = 300 nm and w_k given in Table 2, to make the ratio below 0.05, we just need $n > 4$. In other words, if we keep the first 2×5+1 = 11 Fourier coefficients, the first ignored term only causes a relative error less than 0.05, and the following terms vanish rapidly (which tend to cancel each other because they are related to high-frequency oscillations). Note that a similar conclusion has been drawn in previous statistical studies [4, 12, 13], but ours is based on an analytical approach. Also, from Eq. (12), we can see that the sufficiency of a low-dimensional representation is mainly due to the exponential term, that is, the rapid decay of the Fourier coefficients of the CIE color matching functions. This agrees to the finding of the low pass nature of the human vision system [1].

Improving Performance by Re-sampling

When multiplying spectra, the Fourier coefficients of the product can be directly calculated from those of the factor functions (based on that multiplication of signals is equivalent to convolution of their Fourier transforms), but the computation is not efficient because it is $O(N^2)$, where N is the coefficient number. Moreover, consider multiplying a spiky and a smooth spectrum. Assuming that

$$S_1'(\lambda) = S_1(\lambda) + \sum_{m=1}^{M} w_m \delta(\lambda - l_m), \quad (13)$$

is spiky with $S_1(\lambda)$ as its smooth background and that $S_2(\lambda)$ is smooth, then

$$\begin{aligned} S_1'(\lambda)S_2(\lambda) &= S_1(\lambda)S_2(\lambda) + S_2(\lambda)\sum_{m=1}^{M} w_m \delta(\lambda - l_m) \\ &= S_1(\lambda)S_2(\lambda) + \sum_{m=1}^{M} S_2(l_m) w_m \delta(\lambda - l_m). \end{aligned} \quad (14)$$

This means that we need to know $S_2(l_m)$, the value of $S_2(\lambda)$ at spike location l_m. However, computing $S_2(l_m)$ using the Fourier coefficients of $S_2(\lambda)$ involves evaluating a number of sine and cosine functions, which will significantly slow down the computation.

To improve the performance, we propose to *re-sample* smooth spectra that are reconstructed with Fourier coefficients. Suppose $S(\lambda)$ is reconstructed with 2*N*+1 coefficients $a_0,...,a_N$ and $b_1,...,b_N$. Then the highest frequency involved is N/L. According to the Shannon sampling theorem, the re-sampling interval in the visible range should be less than $L/(2N+1)$ to avoid information loss. To meet this requirement, we simply need to take 2*N*+2 sample points

$$S(\lambda_i) = S(i\Delta\lambda + \lambda_{\min}), \quad i = 1,2,...,2N+2 \quad (15)$$

where $\Delta\lambda = L/(2N+1)$. Thus, a product between two smooth spectra can be obtained through

$$S_3(\lambda_i) = S_1(\lambda_i)S_2(\lambda_i), \quad i = 1,...,2N+2 \qquad (16)$$

which only involves $2N$+2 multiplications. When multiplying a spiky and a smooth spectrum, the functional value $S_2(l_m)$ that appears in Eq. (14) can be determined by a linear interpolation

$$S(l_m) = \frac{(l_m - \lambda_i)}{\Delta\lambda} S(\lambda_i) + \frac{(\lambda_{i+1} - l_m)}{\Delta\lambda} S(\lambda_{i+1}), \qquad (17)$$

where l_m is located within the sampling interval $[\lambda_i, \lambda_{i+1}]$. Overall, we have achieved the linear performance.

Implementation

It is straightforward to implement the re-sampled smooth spectra with arrays and spikes with linked lists. Given any spectrum, it is easy to separate spikes from the smooth part, for example, by use of the gradient information [5]. Sometimes, as measured results, the data for the smooth and spiky parts are already stored separately, such as the fluorescent SPDs [22]. The separtion can be done before any application, i.e. off-line. Finally, if spikes are generated during an application, such as in rendering light dispersion or diffraction, we know that they occur at the object surfaces that cause such optical phenomena and thus add the corresponding spikes to the spike list for the outgoing SPDs.

Tables 3 and 4 display the representing data for the SPDs of Source C, a mercury arc lamp, and a sodium lamp.

Table 3: Fourier coefficients of the smooth part of real spectra.

	a0	a1	b1	a2	b2	a3	b3	a4	b4	a5	b5
Source C	199	-5	16	-8	5	-7	-3	-2	1	-4	-1
Mercury	69	2	2	12	14	-6	2	1	5	-1	0
Sodium	0	0	0	0	0	0	0	0	0	0	0

Table 4: The spikes of real spectra.

	List of locations and weights of all spikes
Source C	
Mercury	(404.7, 5.1), (435.8, 10.4), (491.6, 0.3), (546.1, 13.7), (577.8, 19.3), (693.8, 2.3)
Sodium	(589.0, 31.95)

In summary, the composite model is able to meet all representation criteria. The decomposition allows us to represent arbitrary spectra through a small number of parameters while maintaining good accuracy, and the re-sampling enables us to achieve linear performance. Also in this model, the parameters are portable and easy to adjust for tradeoffs between accuracy and compactness.

Note that the idea of separating impulses from the smooth background was previously proposed by Sharma and Trusell [17] to abstract correct fluorescent spectral data from noisy measurement. But in this paper, the decomposition is based on the general representation criteria for various application areas. (Further mathematical and physical considerations behind the composite model can be found in [19].) Furthermore, this paper proves the sufficiency of a low-dimensional representation and proposes the re-sampling technique, which provide the theoretical foundation and practical efficiency.

Applications

Image Synthesis

Most rendering techniques are *color-based*, which describes lights and objects with RGB triplets typically. However, this approach is not only limited in accuracy [10], but also incapable of handling fluorescent illumination and special optical phenomena such as light dispersion, interference and diffraction. To eliminate these drawbacks, considerable effort has been made on spectral rendering where spectra are represented with sampling [3, 9], linear models [14], and polynomials [7, 15]. However, new problems arise due to the limitations of these methods, as shown in Talbe 1. Now the composite model meets all representation criteria and therefore will advance the research [18].

As an application example, Figure 3 displays images of colorless and colored diamonds that are rendered based on the composite model. Both images demonstrate rainbow-like colors due to light dispersion. Using the composite model, light dispersion can be generated in a straightforward way with a ray tracer. That is, we only need to spawn a series of dispersed monochromatic rays when a light ray enters a dispersive object (such as the diamond), and each monochromatic ray can be perfectly represented with a spike in the composite model.

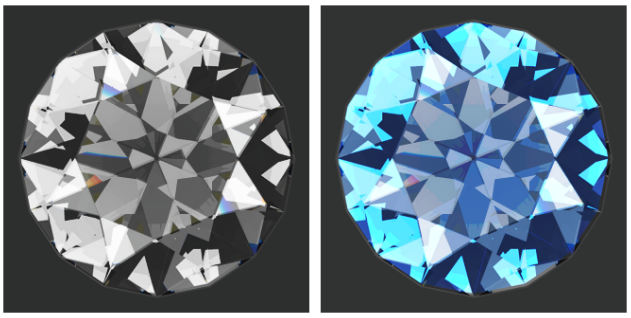

Figure 3: Rendered images of a colorless (left) and colored diamond (right) based on the composite model.

Image Understanding

Spectral images (every pixel provides a SPD) are easier to analyze than color images. Consider the determination of inter-object reflections. At a pixel where one object reflects another, the outgoing SPD $S_3(\lambda)$ is provided by this pixel, the reflectance $S_2(\lambda)$ by some nearby pixels, and the incident SPD $S_1(\lambda)$ by the pixels where the reflected object is located. Thus one can verify whether or not Eq. (1) is

satisfied to determine an inter-object reflection. However, a spectral image requires much more storage space than a color image, and the composite model is appropriate for representing such images because it is compact.

To determine inter-object reflections in a color image, because for colors we do not have a verification equation corresponding to Eq. (1), a reliable judgment has to rely on coherent and consistent conditions for many pixels, which makes the problem difficult. So far color image analysis has not been sufficiently successful [11]. But it is clear that a robust solution relies on accurate spectral relationships and the composite model provides such a basis.

Storage and Communication of Spectral Images

Spectral images have become available from measurement in recent years [20]. One problem of spectral images is that they require a great deal of data to represent, which is disadvantageous for storage and communication. Because the composite model is both accurate and compact, it optimizes the storage and communication of spectral images. Consider a spectral image for a scene involving fluorescent lights. To represent a SPD from 380 nm to 780 nm with the sampling method, at least 400 sample points should be used to avoid missing any spikes. But using the composite model only about 20 parameters (12 for the smooth background and 8 for spikes) are needed. The composite model remarkably improves the compactness.

Deriving Spectra from Colors

In practice, it is very likely that an application needs some spectra but their data are not available. An effective solution is to derive the missing spectra from colors. A simple approach is to assume that a smooth spectrum only contains the three lowest Fourier components [6, 8, 21]. According to Eq. (7), this corresponds to

$$\frac{a_0\bar{a}_{0,k}}{4} + a_1\bar{a}_{1,k} + b_1\bar{b}_{1,k} = X_k, \quad k = 1,2,3 \qquad (18)$$

where $\bar{a}_0$, $\bar{a}_1$, $\bar{b}_1$, and X_k are known and a_0, a_1 and b_1 of the spectrum are to be solved. In deriving the reflectance or transmittance of a material, the accuracy can be improved by use of the material's appearance colors under *different* illuminatants whose SPDs are known. For example, if we know the appearance colors under source A and C, we can determine the six lowest Fourier coefficients using the six independent conditions (three for each appearance color).

With the composite model, it is even possible to use color information to derive SPDs in a scene that contains fluorescent sources. Here we can rely on the fact that the SPDs of fluorescent sources typically have four spikes and they have fixed wavelengths [22]. When lights are reflected and transmitted, the spike number and locations remain the same and only their weights change. Therefore, we have four additional unknown parameters for the spike weights and they, in combination with the unknown parameters for the smooth background, can be solved together through multiple color equations.

Other Applications

The composite model is initiated to represent spectra in the visible range, but it is equally applicable to spectra in other ranges such as infrared or X-ray spectra, as well as other physical signals. This generality is a consequence of the model's physical foundation [19]. Besides, the composite model provides an effective way to represent *absorption spectra*, which contain a smooth background with *negative* spikes (due to discrete absorption). Absorption spectra are very important in physics and chemistry for characterizing materials, but it is impossible to represent them with previous spectral models. However, with composite model, using negative weights for the delta-functions can represent absorption spectra very easily. Finally, the composite model provides a useful basis and constraints for color studies such as color constancy, synthesis and analysis.

Conclusions

In conclusion, we have proposed a composite model to represent spectra by decomposing them into smooth components and spikes. We represent a smooth component through its Fourier coefficients and a spike through its location and height. The composite model satisfies all of the identified representation criteria, and shows promise in several research areas including image synthesis, image understanding, storage and communication of spectral images, and deriving natural spectra.

As future research, it is interesting to apply the composite model in various application areas. For the composite model itself, we can examine different representation candidates for both the smooth and spiky parts. For example, we can represent the smooth part with a wavelet-based expansion, and spikes with narrow Gaussian functions to allow finite widths and heights. Also, the wavelength range can be extended beyond the visible range. In particular, including the ultra-violet region is necessary when a scene involves fluorescent materials, which typically transform ultra-violet light into visible light.

Although the composite model demonstrates significant advantages, one should remember that other spectral models would still be effective in special application areas. For example, in color studies where light sources and objects are restricted, the linear model can be more effective because it's basis functions are specifically adapted according to the spectral domain. However, in solving problems with an open spectral domain such as in image synthesis and analysis, where we do not have a control of the involved spectra, the composite model is more appropriate to use.

Appendix

Now we analytically derive the Fourier coefficients $\bar{a}_{n,k}$ and $\bar{b}_{n,k}$ of the CIE color matching functions. According to Fourier transforms, they are given by

$$\begin{cases} \bar{a}_{n,k} = \dfrac{2}{L}\displaystyle\int_{\lambda_{\min}}^{\lambda_{\max}} \bar{x}_k(\lambda)\cos\left[\dfrac{2\pi n(\lambda-\lambda_{\min})}{L}\right]d\lambda \\ \bar{b}_{n,k} = \dfrac{2}{L}\displaystyle\int_{\lambda_{\min}}^{\lambda_{\max}} \bar{x}_k(\lambda)\sin\left[\dfrac{2\pi n(\lambda-\lambda_{\min})}{L}\right]d\lambda \end{cases} \quad (A.1)$$

Since $\bar{x}_k(\lambda)$ are negligibly small outside $[\lambda_{\min}, \lambda_{\max}]$, we can expand the integral interval to $[-\infty,+\infty]$. Replacing $\bar{x}_k(\lambda)$ with the fit Gaussians shown in Eq. (8), we obtain

$$\begin{cases} \bar{a}_{n,k} = \dfrac{2h_k}{L}\displaystyle\int_{-\infty}^{+\infty} e^{-4(\ln 2)(\lambda-\lambda_{c,k})^2/w_k^2}\cos\left[\dfrac{2\pi n(\lambda-\lambda_{\min})}{L}\right]d\lambda \\ \bar{b}_{n,k} = \dfrac{2h_k}{L}\displaystyle\int_{-\infty}^{+\infty} e^{-4(\ln 2)(\lambda-\lambda_{c,k})^2/w_k^2}\sin\left[\dfrac{2\pi n(\lambda-\lambda_{\min})}{L}\right]d\lambda \end{cases} \quad (A.2)$$

for $k = 2,3$ and similar results for $k = 1$. Substituting $\lambda = \lambda + \lambda_{c,k}$, $\alpha^2 = 4(\ln 2)/w_k^2$, $\beta = 2\pi n/L$, $\gamma = 2h_k/L$, and $\lambda' = \lambda_{c,k} - \lambda_{\min}$, Eq. (A.2) becomes

$$\begin{cases} \bar{a}_{n,k} = 2\gamma\cos(\beta\lambda')\displaystyle\int_0^{+\infty} e^{-\alpha^2\lambda^2}\cos(\beta\lambda)d\lambda, \quad n = 0,1,...,\infty \\ \bar{b}_{n,k} = 2\gamma\sin(\beta\lambda')\displaystyle\int_0^{+\infty} e^{-\alpha^2\lambda^2}\cos(\beta\lambda)d\lambda, \quad n = 1,2,...,\infty \end{cases} \quad (A.3)$$

where we have used the fact that $\cos(\beta\lambda)$ is even and $\sin(\beta\lambda)$ is odd over $[-\infty,+\infty]$. Since

$$\int_0^{+\infty} e^{-\alpha^2\lambda^2}\cos(\beta\lambda)d\lambda = \frac{\sqrt{\pi}}{2\alpha}e^{-\beta^2/4\alpha^2}, \quad (A.4)$$

we obtain

$$\begin{cases} \bar{a}_{n,k} = \dfrac{\sqrt{\pi}\gamma\cos(\beta\lambda')}{\alpha}e^{-\beta^2/4\alpha^2}, \quad n = 0,1,...,\infty \\ \bar{b}_{n,k} = \dfrac{\sqrt{\pi}\gamma\sin(\beta\lambda')}{\alpha}e^{-\beta^2/4\alpha^2}, \quad n = 1,2,...,\infty \end{cases} \quad (A.5)$$

Substituting with the original parameters, the final results for $k = 2,3$ are

$$\begin{cases} \bar{a}_{n,k} = \dfrac{\sqrt{\pi}h_k w_k}{\sqrt{\ln 2}L}\cos\left[\dfrac{2\pi n(\lambda_{c,k}-\lambda_{\min})}{L}\right]e^{-(\pi n w_k)^2/4(\ln 2)L^2} \\ \bar{b}_{n,k} = \dfrac{\sqrt{\pi}h_k w_k}{\sqrt{\ln 2}L}\sin\left[\dfrac{2\pi n(\lambda_{c,k}-\lambda_{\min})}{L}\right]e^{-(\pi n w_k)^2/4(\ln 2)L^2} \end{cases} \quad (A.6)$$

For $k = 1$, the coefficients have similar expressions except that each will contain two terms corresponding to the two Gaussians.

References

1. H. B. Barlow, "What causes trichromacy? A theoretical analysis using comb-filtered spectra," *Vision Res.* **22**, 635-643 (1982).
2. D. H. Brainard and B. A. Wandell, "Calibrated processing of image color," *Color Res. Appl.* **15**, 266-271 (1990).
3. R. L. Cook and K. E. Torrance, "A reflection model for computer graphics," *ACM Trans. on Graphics* **1**, 7-24 (1982).
4. J. L. Dannemiller, "Spectral reflectance of natural objects: how many basis functions are necessary," *J. Opt. Soc. Am.* **A9**, 507-515 (1992).
5. P. M. Deville, S. Merzouk, D. Cazier, and J. C. Paul, "Spectral data modeling for a lighting application", *Computer Graphics Forum* **13(3)**, 97-106 (1994).
6. M. Drew and B. Funt, "Natural metamers," *CVGIP: Image Understanding* **56**, 139-151 (1992).
7. R. Geist, O. Heim, and S. Junkins, "Color representation in virtual environments," *Color Res. Appl.* **21**, 121-128 (1996).
8. A. S. Glassner, "How to derive a spectrum from an RGB triplet," *IEEE Computer Graphics & Appl.* **9(4)**, 95-99 (1989).
9. J. S. Gondek, G. W. Meyer, J. G. Newman, "Wavelength dependent reflection functions," *Computer Graphics*, *Proc. of ACM SIGGRAPH 94*, ACM Press, New York, 213-219 (1994).
10. R. Hall and D. P. Greenberg, "A testbed for realistic image synthesis," *IEEE Computer Graphics & Appl.* **3**, 10-20 (1983).
11. G. J. Klinker, *A Physical Approach to Color Image Understanding*, A K Peters, Massachusetts, 1993.
12. L. T. Maloney, "Evaluation of linear models of surface spectral reflectance with small numbers of parameters," *J. Opt. Soc. Am.* **A3**, 1673-1683 (1986).
13. J. P. S. Parkkinen, J. Hallikainen, and T. Jaaskelainen, "Characteristic spectra of Munsell colors," *J. Opt. Soc. Am.* **A6**, 318-322 (1989).
14. M. S. Peercy, "Linear color representations in full spectral rendering," in *Computer Graphics*, *Proc. of SIGGRAPH 93*, 191-198 (1993).
15. M. Raso and A. Fournier, "A piecewise polynomial approach to shading using spectral distributions," in *Graphics Interface 91*, 40-46 (1991).
16. G. Rougeron and B. Peroche, "Color fidelity in computer graphics: A survey," *Computer Graphics Forum*, **17(1)**, 3-15 (1998).
17. G. Sharma and H. J. Trusell, "Decomposition of fluorescent illuminant spectra for accurate colorimetry," in *IEEE-ICIP*, 1002-1006 (1994).
18. Y. Sun, "A spectrum-based framework for realistic image synthesis," *Ph.D. Thesis*, *Simon Fraser University,* 2000. Available at ftp://fas.sfu.ca/pub/cs/theses/2000/.
19. Y. Sun, F. D. Fracchia, and M. S. Drew, "A physically-based dual representation of spectral functions," to appear in *Optical Engineering*, Nov., 2000.
20. P. L. Vora, M. L. Harvill, J. E. Farrell, J. D. Tietz, and D. H. Brainard, "Image capture: synthesis of sensor responses from multispectral images," in *Proc. of the 1997 IS&T/SPIE Conf. On Electronic Imaging*, (1997).
21. B. A. Wandell, "The synthesis and analysis of color images," *IEEE Trans. Pattern Anal. Mach. Intelligence* **9(1)**, 2-13 (1987).
22. G. Wyszecki and W. Stiles, *Color Science: Concepts and Methods, Quantitative Data and Formulas*, Second Edition, Wiley, New York (1982).